Chapter

Quantum Theory of the Seebeck Coefficient in YBCO

Shigeji Fujita and Akira Suzuki

Abstract

The measured in-plane thermoelectric power (Seebeck coefficient) S_{ab} in YBCO below the superconducting temperature T_c (∼94 K) S_{ab} is negative and T-independent. This is shown to arise from the fact that the "electrons" (minority carriers) having heavier mass contribute more to the thermoelectric power. The measured out-of-plane thermoelectric power S_c rises linearly with the temperature T. This arises from moving bosonic pairons (Cooper pairs), the Bose-Einstein condensation (BEC) of which generates a supercurrent below T_c. The center of mass of pairons moves as bosons. The resistivity ρ_{ab} above T_c has T-linear and T-quadratic components, the latter arising from the Cooper pairs being scattered by phonons.

Keywords: Seebeck coefficient, in-plane thermoelectric power, out-of-plane thermoelectric power, moving bosonic pairons (Cooper pairs), Bose-Einstein condensation, supercurrent, YBCO

1. Introduction

In 1986, Bednorz and Müller [1] reported their discovery of the first of the high-T_c cuprate superconductors (La-Ba-Cu-O, $T_c > 30$ K). Since then many investigations [2, 3] have been carried out on high-T_c superconductors (HTSC) including Y-Ba-Cu-O (YBCO) with $T_c \sim 94$ K [4]. These compounds possess all of the main superconducting properties, including zero resistance, Meissner effect, flux quantization, Josephson effect, gaps in the excitation energy spectra, and sharp phase transition. In addition these HTSC are characterized by (i) two-dimensional (2D) conduction, (ii) short zero-temperature coherence length ξ_0 (∼ 10Å), (iii) high critical temperature T_c (∼ 100 K), and (iv) two energy gaps. The transport behaviors above T_c are significantly different from those of a normal metal.

YBCO has a critical (superconducting) temperature $T_c \sim 94$ K, which is higher than the liquid nitrogen temperature (77 K). This makes it a very useful superconductor. Terasaki et al. [5, 6] measured the resistivity ρ, the Hall coefficient R^H, and the Seebeck coefficient (thermoelectric power) S in YBCO above the critical temperature T_c. A summary of the data is shown in **Figure 1**. In-plane Hall coefficient R^H_{ab} is positive and temperature (T)-independent, while in-plane Seebeck coefficient S_{ab} is negative and T-independent (anomaly). Thus, there are different charge carriers for the Ohmic conduction and the thermal diffusion. We know that the carrier's mass is important in the Ohmic currents. Lighter mass particles contribute more to the conductivity. The T independence of R^H_{ab} and S_{ab} suggests that "electrons" and "holes" are responsible for the behaviors. We shall explain this behavior,

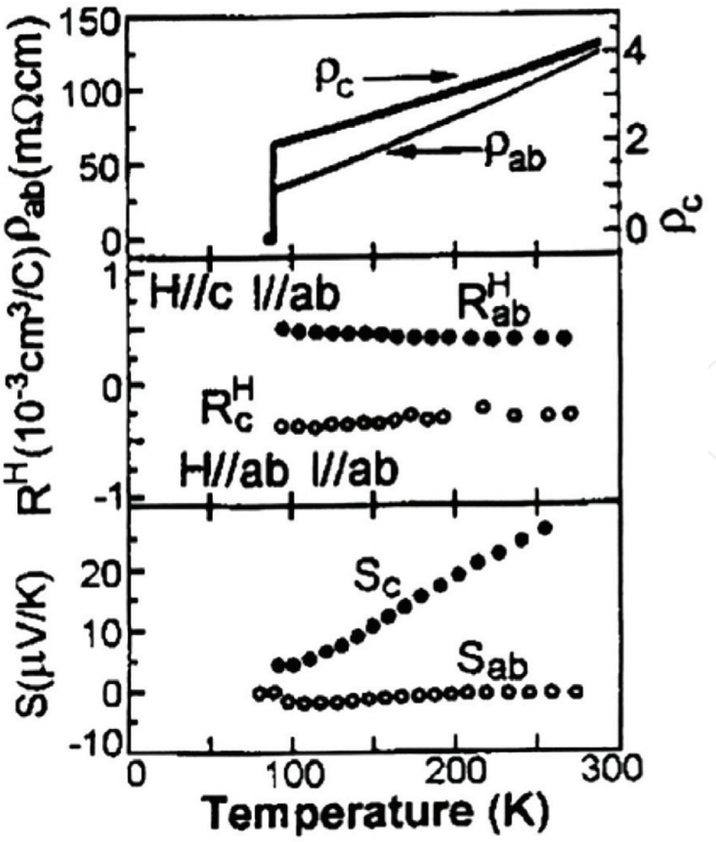

Figure 1.
Normal-state transport of highly oxygenated $YBa_2Cu_3O_{7-\delta}$ after Terasaki et al.'s [5, 6]. Resistivities (top panel); Hall coefficients (middle panel); Seebeck coefficient (bottom panel). The subscripts ab and c denote in-copper plane and out-of-plane directions, respectively.

by assuming "electrons" and "holes" as carriers and using statistical mechanical calculations. Out-of-plane Hall coefficient R_c^H is negative and temperature-independent, while out-of-plane Seebeck coefficient S_c is roughly temperature (T)-linear. We shall show that the pairons, whose Bose condensation generates the supercurrents below T_c, are responsible for this strange T-linear behavior. The in-plane resistivity appears to have T-linear and T-quadratic components. We discuss the resistivity ρ above the critical temperature T_c in Section 6.

In this paper we are mainly interested in the sign and the temperature behavior of the Seebeck coefficient in YBCO. But we discuss the related matter for completeness. There are no Seebeck currents in the superconducting state below the critical temperature $(S = 0)$.

2. The crystal structure of YBCO: two-dimensional conduction

HTSC have *layered structures* such that the copper planes comprising Cu and O are periodically separated by a great distance (e.g., $a = 3.88$ Å, $b = 3.82$ Å, $c = 11.68$ Å for YBCO). The lattice structure of YBCO is shown in **Figure 2**. The succession of layers along the c-axis can be represented by CuO–BaO–CuO_2–Y-CuO_2–BaO-CuO–[CuO–BaO–...]. The buckled CuO_2 plane where Cu-plane and O-plane are separated by a short distance as shown is called the *copper planes*. The two copper planes separated by yttrium (Y) are about 3 Å apart, and they are believed to be responsible for superconductivity.

The conductivity measured is a few orders of magnitude smaller along the c-axis than perpendicular to it [7]. This appears to contradict the prediction based on the

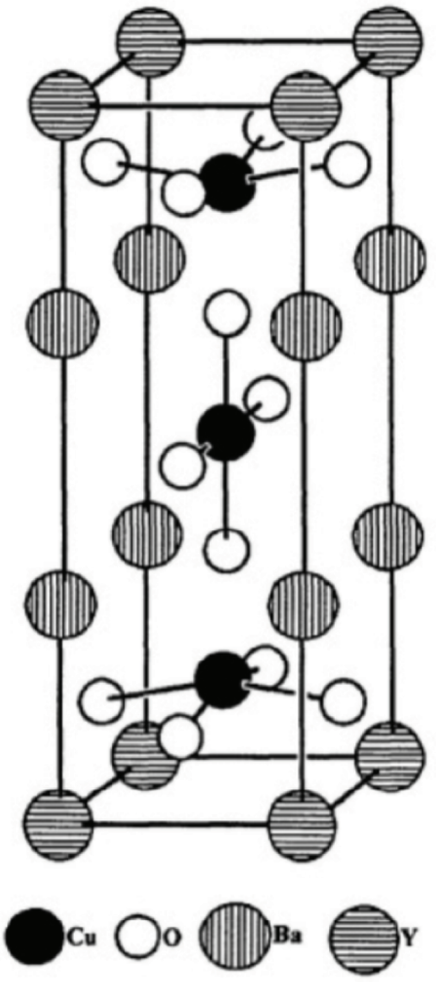

Figure 2.
Arrangement of atoms in a crystal of $YBa_2Cu_3O_7$.

naive application of the Bloch theorem. This puzzle may be solved as follows [8]. Suppose an electron jumps from one conducting layer to its neighbor. This generates a change in the charge states of the layers involved. If each layer is macroscopic in dimension, we must assume that the charge state Q_n of the nth layer can change without limits: $Q_n = \ldots, -2, -1, 0, 1, 2, \ldots$ in units of the electron charge (magnitude) e. Because of unavoidable short circuits between layers due to lattice imperfections, these Q_n may not be large. At any rate if Q_n are distributed *at random* over all layers, then the periodicity of the potential for electron along the c-axis is destroyed. The Bloch theorem based on the electron potential periodicity does not apply even though the lattice is periodic along the c-axis. As a result there are *no* k-vectors along the c-axis. This means that the effective mass in the c-axis direction is infinity, so that *the Fermi surface for a layered conductor is a right cylinder with its axis along the c-axis*. Hence a 2D conduction is established.

Since electric currents flow in the copper planes, there are continuous k-vectors and Fermi energy ε_F. Many experiments [1–3, 9] indicate that a singlet pairs with antiparallel spins called *Cooper pairs* (pairons) form a supercondensate below T_c.

Let us first examine the cause of electron pairing. We first consider attraction via the longitudinal acoustic phonon exchange. Acoustic phonons of lowest energies have long wavelengths λ and a linear energy-momentum (ε-$\hbar k$) relation:

$$\varepsilon = c_s \hbar k, \tag{1}$$

may be assumed, where c_s is the sound speed. The attraction generated by the exchange of longitudinal acoustic phonons is long-ranged. This mechanism is good

for a type I superconductor whose pairon size is of the order of 10^4 Å. This attraction is in action also for a HTSC, but it alone is unlikely to account for the much smaller pairon size.

Second we consider the optical phonon exchange. Roughly speaking each copper plane has Cu and O, and 2D lattice vibrations of optical modes are expected to be important. Optical phonons of lowest energies have short wavelengths of the order of the lattice constants, and they have a quadratic dispersion relation:

$$\varepsilon = \varepsilon_0 + A_1\left(k_1 - \frac{\pi}{a_1}\right)^2 + A_2\left(k_2 - \frac{\pi}{a_2}\right)^2, \tag{2}$$

where ε_0, A_1, and A_2 are constants. The attraction generated by the exchange of a massive boson is short-ranged just as the short-ranged nuclear force between two nucleons generated by the exchange of massive pions, first shown by Yukawa [10]. Lattice constants for YBCO are given by $(a_1, a_2) = (3.88, 3.82)$ Å, and the limit wavelengths $(\lambda_{\min})$ at the Brillouin boundary are twice these values. The observed coherence length ξ_0 is of the same order as $\lambda_{\min}$:

$$\xi_0 \sim \lambda_{\min} \simeq 8\text{Å}. \tag{3}$$

Thus an electron-optical phonon interaction is a viable candidate for the cause of the electron pairing. To see this in more detail, let us consider the copper plane. With the neglect of a small difference in lattice constants along the a- and b-axes, Cu atoms form a square lattice of a lattice constant $a_0 = 3.85$ Å, as shown in **Figure 3**. Twice as many oxygen (O) atoms as copper (Cu) atoms occupy midpoints of the nearest neighbors (Cu, Cu) in the x_1-x_2 plane.

First, let us look at the motion of an electron wave packet that extends over more than one Cu-site. This wave packet may move easily in $\langle 110 \rangle$ rather than the first neighbor directions [100] and [010]. The Bloch wave packets are superposable; therefore, the electron can move in any direction characterized by the two-dimensional k-vectors with bases taken along [110] and $[1\bar{1}0]$. If the number density of electrons is small, the Fermi surfaces should then be a small circle as shown in the central part in **Figure 4**.

Second, we consider a hole wave packet that extends over more than one O-site. It may move easily in $\langle 100 \rangle$ because the Cu-sublattice of a uniform charge

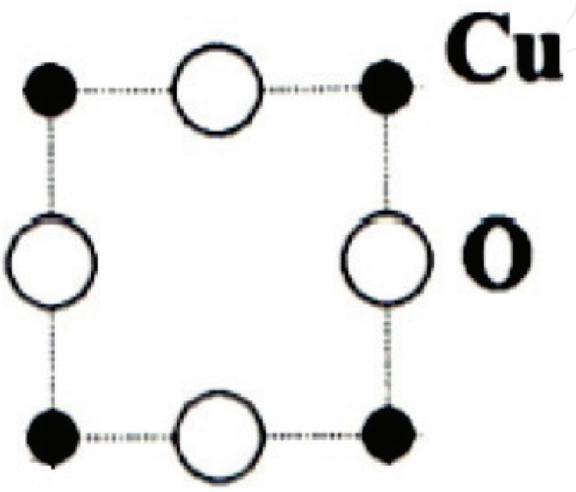

Figure 3.
The idealized copper plane contains twice as many O's as Cu's.

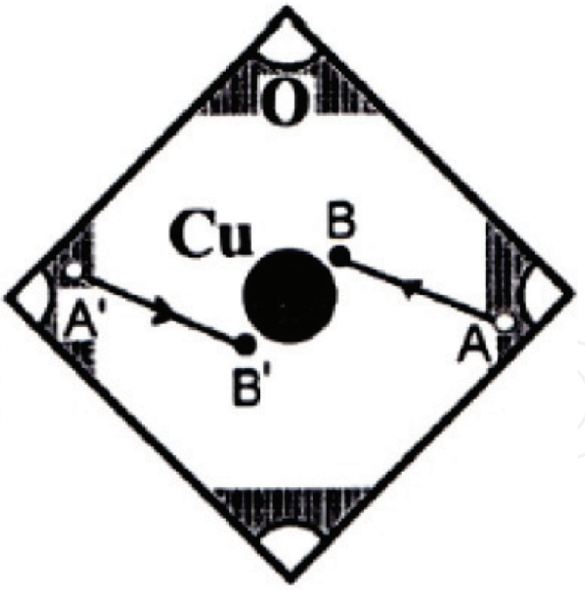

Figure 4.
The two-dimensional Fermi surface of a cuprate model has a small circle (electrons) at the center and a set of four small pockets (holes) at the Brillouin boundary. Exchange of a phonon can create the electron pairon at (B, B') and the hole pairon at (A, A'). The phonon must have a momentum $p \equiv \hbar k$, with k being greater than the distance between the electron circle and the hole pockets.

distribution favors such a motion. If the number of holes is small, the Fermi surface should consist of the four small pockets shown in **Figure 4**. Under the assumption of such a Fermi surface, pair creation of $\pm$ pairons via an optical phonon may occur as shown in the figure. Here a single-phonon exchange generates an electron transition from A in the O-Fermi sheet to B in the Cu-Fermi sheet and another electron transition from A′ to B′, creating the $-$pairon at $(\mathrm{B}, \mathrm{B}')$ and the +pairon at $(\mathrm{A}, \mathrm{A}')$. From momentum conservation the momentum (magnitude) of a phonon must be equal to $\hbar$ times the k-distance AB, which is approximately equal to the momentum of an optical phonon of the smallest energy. Thus an almost insulator-like layered conductor should have a Fermi surface comprising a small electron circle and small hole pockets, which are quite favorable for forming a supercondensate by exchanging an optical phonon.

3. Quantum statistical theory of superconductivity

Following the Bardeen, Cooper, and Schrieffer (BCS) theory [11], we regard the phonon-exchange attraction as the cause of superconductivity. Cooper [12] solved Cooper's equation and obtained a linear dispersion relation for a moving pairon:

$$\varepsilon = w_0 + \frac{1}{2} v_{\mathrm{F}} p, \tag{4}$$

where w_0 is the ground-state energy of the Cooper pair (pairon) and v_{F} is the Fermi speed. This relation was obtained for a three-dimensional (3D) system. For a 2D system, we obtain

$$\varepsilon = w_0 + \frac{2}{\pi} v_{\mathrm{F}} p. \tag{5}$$

The center of mass (CM) motion of a composite is bosonic (fermionic) according to whether the composite contains an even (odd) number of elementary

fermions. The Cooper pairs, each having two electrons, move as bosons. In our quantum statistical theory of superconductivity [13], the superconducting temperature T_c is regarded as the Bose-Einstein condensation (BEC) point of pairons. The center of mass of a pairon moves as a boson [13]. Its proof is given in Appendix for completeness. The critical temperature T_c in 2D is given by

$$k_B T_c = 1.24 \hbar v_F n^{1/2}, \tag{6}$$

where n is the pairon density. The inter-pairon distance

$$r_0 \equiv n^{-1/2} = 1.24 \hbar v_F (k_B T_c)^{-1} \tag{7}$$

is several times greater than the BCS pairon size represented by the BCS coherence length:

$$\xi_0 \equiv 0.181 \hbar v_F (k_B T_c)^{-1}. \tag{8}$$

Hence the BEC occurs without the pairon overlap. Phonon exchange can be repeated and can generate a pairon-binding energy ε_b of the order of $k_B T_b$:

$$\varepsilon_b \equiv k_B T_b, \quad T_b \sim 1000 \text{ K}. \tag{9}$$

Thus, the pairons are there above the superconducting temperature T_c. The angle-resolved photoemission spectroscopy (ARPES) [14] confirms this picture.

In the quantum statistical theory of superconductivity, we start with the crystal lattice, the Fermi surface and the Hamiltonian and calculate everything, using statistical mechanical methods. The details are given in Ref. [15].

Loram et al. [15] extensively studied the electronic heat capacity of $YBa_2CuO_{6+\delta}$ with varying oxygen concentrations $6 + \delta$. A summary of their data is shown in **Figure 5**. The data are in agreement with what is expected of a Bose-Einstein (B-E)

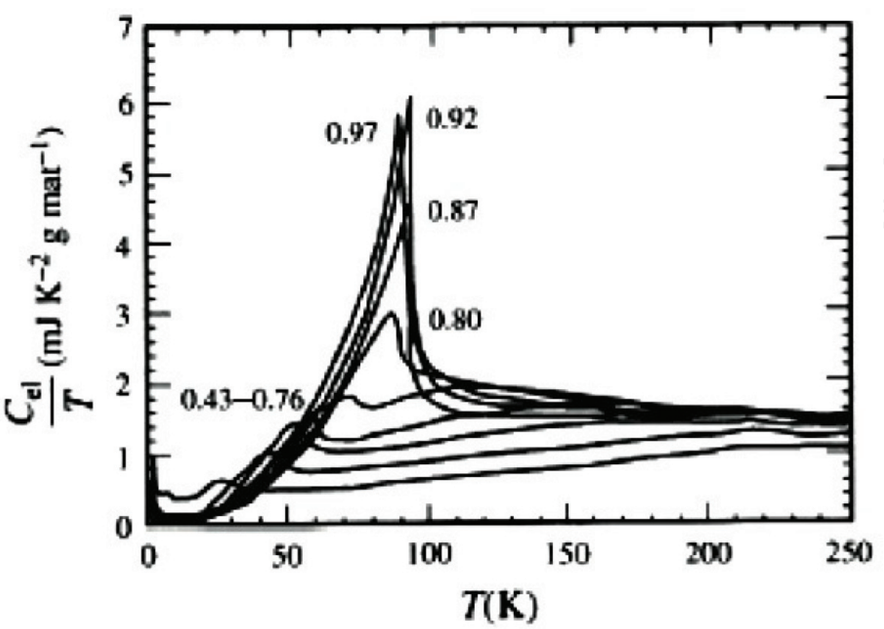

Figure 5.
Electronic heat capacity C_{el} plotted as C_{el}/T vs. temperature T after Loram et al. [15] for $YBa_2Cu_3O_{6+\delta}$ with the δ values shown.

condensation of free massless bosons in 2D, a peak with no jump at T_c with the T^2-law decline on the low-temperature side. The maximum heat capacity at T_c with a shoulder on the high-temperature side can only be explained naturally from the view that the superconducting transition is a macroscopic change of state generated by the participation of a great number of pairons with no dissociation. The standard BCS model regards their T_c as the pair dissociation point and predicts no features above T_c.

The molar heat capacity C for a 2D massless bosons rises like T^2 in the condensed region and reaches $4.38R$ at $T = T_c$; its temperature derivative $\partial C(T,n)/\partial T$ jumps at this point. The *order of phase transition* is defined to be that order of the derivative of the free energy F whose discontinuity appears for the first time. Since $C_V = T(\partial S/\partial T)_V = -T\left(\partial^2 F/\partial T^2\right)$, $\partial C_V/\partial T = -T\left(\partial^3 F/\partial T^3\right) - \left(\partial^2 F/\partial T^2\right)$, the B-E condensation is a *third-order phase transition*. The temperature behavior of the heat capacity C in **Figure 6** is remarkably similar to that of $YBa_2Cu_3O_{6.92}$ (optimal sample) in **Figure 5**. This is an important support for the quantum statistical theory. Other support is discussed in Sections 5 and 6.

Our quantum statistical theory can be applied to 3D superconductors as well. The linear dispersion relation (4) holds. The superconducting temperature T_c in 3D is given by

$$k_B T_c = 1.01\hbar v_F n^{\frac{1}{3}}, \tag{10}$$

which is identified as the BEC point. The molar heat capacity C for 3D bosons with the linear dispersion relation $\varepsilon = cp$ rises like T^3 and reaches $10.8R$, $R =$ gas constant, at $T_c = 2.02\hbar c n_0^{1/3}$. It then drops abruptly by $6.57R$ and approaches $3R$ in the high-temperature limit. This temperature behavior of C is shown in **Figure 7**. The phase transition is of second order. This behavior is good agreement with experiments, which supports the BEC picture of superconductivity.

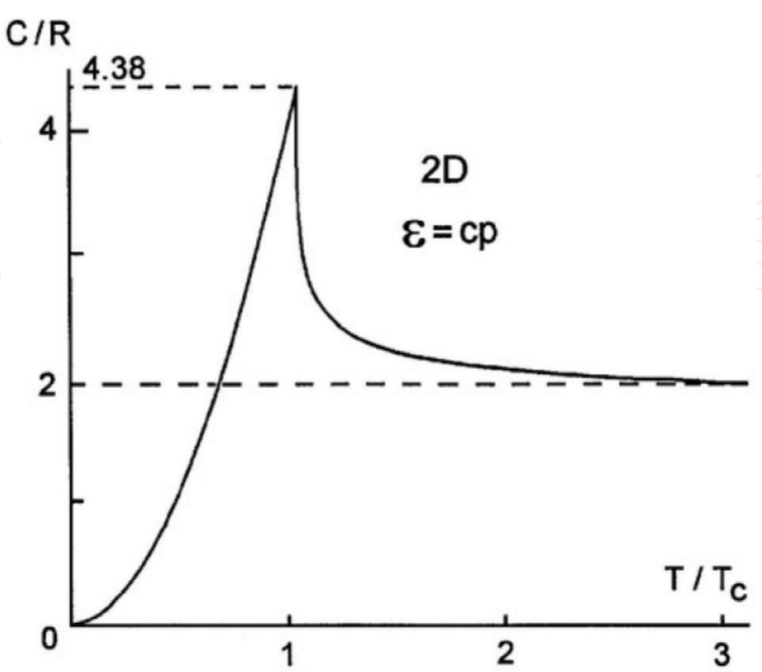

Figure 6.
The molar heat capacity C for 2D massless bosons rise like T^2, reaches 4.38R at the critical temperature T_c, and then decreases to 2R in the high-temperature limit.

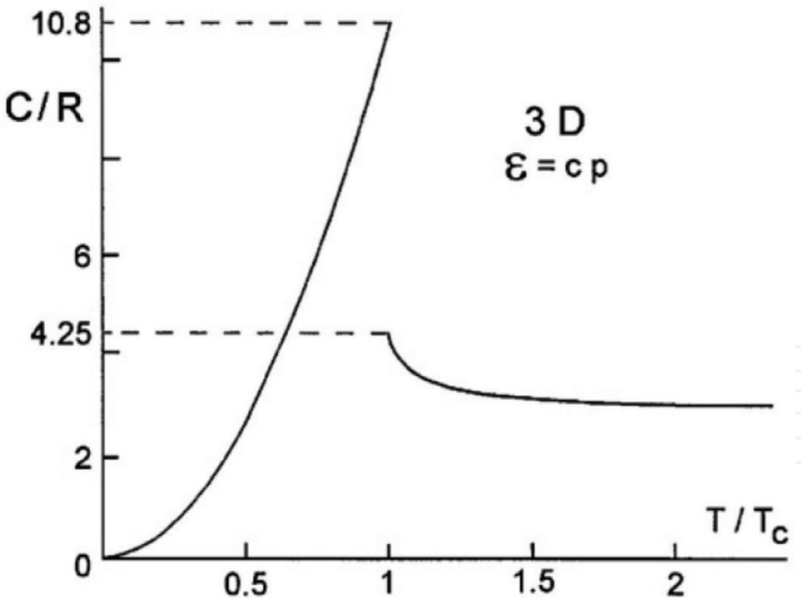

Figure 7.
The molar heat capacity C for 3D massless bosons rises like T^3 and reaches 10.8R at the critical temperature $T_c = 2.02\hbar c n_0^{1/3}$. It then drops abruptly by 6.57R and approaches the high-temperature limit 3R.

4. In-plane Seebeck coefficient above the critical temperature

4.1 Seebeck coefficient for conduction electrons

When a temperature difference is generated and/or an electric field $\boldsymbol{E}$ is applied across a conductor, an electromotive force (emf) is generated. For small potential and temperature gradients, the linear relation between the electric current density $\boldsymbol{j}$ and the gradients

$$\boldsymbol{j} = \sigma(-\nabla V) + A(-\nabla T) = \sigma \boldsymbol{E} - A\nabla T \tag{11}$$

holds, where $\boldsymbol{E} = -\nabla V$ is the electric field and σ is the conductivity. If the ends of the conducting bar are maintained at different temperatures, no electric current flows. Thus from Eq. (11), we obtain

$$\sigma \boldsymbol{E}_S - A\nabla T = 0, \tag{12}$$

where $\boldsymbol{E}_S$ is the field generated by the thermal emf. The Seebeck coefficient S, also called the thermoelectric power or the thermopower, is defined through

$$\boldsymbol{E}_S = S\nabla T, \quad S \equiv A/\sigma. \tag{13}$$

The conductivity σ is always positive, but the Seebeck coefficient S can be positive or negative depending on the materials. We present a kinetic theory to explain Terasaki et al.'s experimental results [5, 6] for the Seebeck coefficient in $YBa_2Cu_3O_{7-\delta}$, reproduced in **Figure 1**.

We assume that the carriers are conduction electrons ("electron," "hole") with charge q ($-e$ for "electron," $+e$ for "hole") and effective mass m^*. At a finite temperature $T > 0$, "electrons" ("holes") are excited near the Fermi surface if the surface curvature is negative (positive) [16]. The "electron" ("hole") is a *quasi-electron* which has an energy higher lower than the Fermi energy ε_F *and* which circulates clockwise (counterclockwise) viewed from the tip of the applied magnetic field vector.

"Electrons" ("holes") are excited on the positive (negative) side of the Fermi surface with the convention that the positive normal vector at the surface points in the energy-increasing direction. The number of thermally excited "electrons" N_{ex}, having energies greater than the Fermi energy ε_{F}, is defined and calculated as

$$\begin{aligned} N_{\text{ex}} &\equiv \int_{\varepsilon_{\text{F}}}^{\infty} \mathrm{d}\varepsilon\, \mathcal{D}(\varepsilon) f(\varepsilon, T, \mu) \approx \mathcal{D}(\varepsilon_{\text{F}}) \int_{\varepsilon_{\text{F}}}^{\infty} \mathrm{d}\varepsilon\, \frac{1}{e^{\beta(\varepsilon-\mu)}+1} \\ &\simeq \ln 2\, k_{\text{B}} T \mathcal{D}(\varepsilon_{\text{F}}), \end{aligned} \tag{14}$$

where $\mathcal{D}(\varepsilon)$ is the density of states. This formula holds for 2D and 3D in high degeneracy. The density of thermally excited "electrons,"

$$n_{\text{ex}} = N_{\text{ex}}/\mathcal{A}, \quad \mathcal{A} = \text{planer area}, \tag{15}$$

is higher at the high-temperature end, and the particle current runs from the high- to the low-temperature end. This means that the electric current runs toward (away from) the high-temperature end in an "electron" ("hole")-rich material. After using Eqs. (13) and (14), we obtain

$$S = \begin{cases} < 0 & \text{for "electrons"} \\ > 0 & \text{for "holes"} \end{cases} \tag{16}$$

The Seebeck current arises from the thermal diffusion. We assume Fick's law:

$$\boldsymbol{j} = q\boldsymbol{j}_{\text{particle}} = -qD\nabla n_{\text{ex}}, \tag{17}$$

where D is the *diffusion constant*, which is computed from the standard formula:

$$D = \frac{1}{\mathrm{d}} v\ell = \frac{1}{\mathrm{d}} v_{\text{F}}^2 \tau, \quad v = v_{\text{F}}, \quad \ell = v\tau, \tag{18}$$

where v_{F} is the Fermi velocity and τ the relaxation time of the charged particles. The symbol d denotes the dimension. The density gradient ∇n_{ex} is generated by the temperature gradient ∇T and is given by

$$\nabla n_{\text{ex}} = \frac{\ln 2}{\mathcal{A}\mathrm{d}} k_{\text{B}} \mathcal{D}(\varepsilon_{\text{F}}) \nabla T, \tag{19}$$

where Eq. (14) is used. Using Eqs. (17)–(19) and (11), we obtain the thermal diffusion coefficient A as

$$A = \frac{\ln 2}{2\mathcal{A}} q v_{\text{F}}^2 k_{\text{B}} \mathcal{D}(\varepsilon_{\text{F}}) \tau. \tag{20}$$

We divide A by the conductivity

$$\sigma = nq^2\tau/m^*, \tag{21}$$

and obtain the Seebeck coefficient S [see Eq. (13)]:

$$S \equiv A/\sigma = \ln 2 \frac{k_{\text{B}}\varepsilon_{\text{F}}}{nq} \frac{\mathcal{D}(\varepsilon_{\text{F}})}{\mathcal{A}}, \quad \varepsilon_{\text{F}} \equiv \frac{1}{2} m^* v_{\text{F}}^2. \tag{22}$$

The relaxation time τ cancels out from numerator and denominator. This result is independent of the temperature T.

4.2 In-plane thermopower for YBCO

We apply our theory to explain the in-plane thermopower data for YBCO. For $YBa_2Cu_3O_{7-\delta}$ (composite), there are "electrons" and "holes". The "holes", having smaller m^* and higher $v_F \equiv (2\varepsilon_F/m^*)^{1/2}$, dominate in the Ohmic conduction and also in the Hall voltage V_H, yielding a positive Hall coefficient R_{ab}^H (see **Figure 1**). But the experiments indicate that the in-plane thermopower S_{ab} is negative. This puzzle may be solved as follows.

We assume an effective mass approximation for the in-plane "electrons":

$$\varepsilon = \left(p_x^2 + P_y^2\right)/2m^*. \tag{23}$$

The 2D density of states including the spin degeneracy is

$$\mathcal{D} = m^* A/\left(\pi\hbar^2\right), \tag{24}$$

which is independent of energy. The "electrons" (minority carriers), having heavier mass m_1^*, contribute more to A, and hence the thermopower S_{ab} can be negative as shown below.

When both "electrons" (1) and "holes" (2) exist, their contributions to the thermal diffusion are additive. Using Eqs. (20) and (24), we obtain

$$\begin{aligned} A_{ab} &= -e\ln 2\,\frac{k_B}{2\pi\hbar^2}\left(v_F^{(1)}\right)^2 m_1^*\,\tau_1 + e\ln 2\,\frac{k_B}{2\pi\hbar^2}\left(v_F^{(2)}\right)^2 m_2^*\,\tau_2 \\ &= -e\ln 2\,\frac{k_B\varepsilon_F}{\pi\hbar^2}(\tau_1 - \tau_2). \end{aligned} \tag{25}$$

If phonon scattering is assumed, then the scattering rate is given by

$$\Gamma \equiv \tau^{-1} = n_{ph} v_F s, \tag{26}$$

where s is the scattering diameter and n_{ph} denotes the phonon population given by the Planck distribution function:

$$n_{ph} = \left[\exp\left(\varepsilon_{ph}/k_B T\right) - 1\right]^{-1}, \tag{27}$$

where ε_{ph} is a phonon energy. We then obtain

$$\begin{aligned} \tau_1 - \tau_2 &= 1/\Gamma_1 - 1/\Gamma_2 = \left(n_{ph} v_F^{(1)} s\right)^{-1} - \left(n_{ph} v_F^{(2)} s\right)^{-1} \\ &= \frac{1}{n_{ph} s}\left(\frac{1}{v_F^{(1)}} - \frac{1}{v_F^{(2)}}\right) > 0, \qquad \left(v_F^{(1)} < v_F^{(2)}\right). \end{aligned} \tag{28}$$

The total conductivity is

$$\begin{aligned} \sigma = \sigma_1 + \sigma_2 &= \frac{e^2 n_1}{m_1^*}\tau_1 + \frac{e^2 n_2}{m_2^*}\tau_2 \\ &= \frac{e^2 n_1}{m_1^* v_F^{(1)} n_{ph} s} + \frac{e^2 n_2}{m_2^* v_F^{(2)} n_{ph} s}. \end{aligned} \tag{29}$$

Using Eqs. (25)–(29), we obtain the in-plane thermopower S_{ab} above the critical temperature as

$$S_{ab} \equiv \frac{A_{ab}}{\sigma_{ab}} = -\ln 2 \frac{k_B \varepsilon_F}{\pi e \hbar^2} \left(\frac{1}{v_F^{(1)}} - \frac{1}{v_F^{(2)}} \right) \left(\frac{n_1}{m_1^* v_F^{(1)}} + \frac{n_2}{m_2^* v_F^{(2)}} \right)^{-1}. \tag{30}$$

The factors $n_{ph}s$ drop out from numerator and denominator. The obtained Seebeck coefficient S_{ab} is negative and T-independent, in agreement with experiments in $YBa_2Cu_3O_{7-\delta}$, reproduced in **Figure 1**.

5. Out-of-plane thermopower

Terasaki et al. [17, 18] and Takenaka et al. [19] measured the out-of-plane resistivity ρ_c in $YBa_2Cu_3O_x$. In the range $6.6 < x < 6.92$, the data for ρ_c can be fitted with

$$\rho_c = C_1 \rho_{ab} + C_2/T, \tag{31}$$

where C_1 and C_2 are constants and ρ_{ab} is the in-plane resistivity. The first term $C_1\rho_{ab}$ arises from the in-plane conduction due to the (predominant) "holes" and + pairons. The second term C_2/T arises from the − pairons' quantum tunneling between the copper planes [20]. Pairons move with a linear dispersion relation [21]:

$$\varepsilon = \begin{cases} \frac{2}{\pi} v_F p \equiv cp, & p < p_0 \equiv |w_0|/c \\ 0, & \text{otherwise} \end{cases} \tag{32}$$

with $|w_0|$ being the binding energy of a pairon. The Hall coefficient R_c^H (current along the c-axis) is observed to be negative, indicating that the carriers have negative charge (see **Figure 1**).

The tunneling current is calculated as follows. A pairon arrives at a certain lattice-imperfection (impurity, lattice defect, etc.) and quantum-jumps to a neighboring layer with the jump rate given by the Dirac-Fermi golden rule

$$w = \frac{2\pi}{\hbar} \left| \langle \boldsymbol{p}_f | U | \boldsymbol{p}_i \rangle \right|^2 \delta(\varepsilon_f - \varepsilon_i) \equiv \frac{2\pi}{\hbar} \mathcal{M}^2 \delta(\varepsilon_f - \varepsilon_i), \tag{33}$$

where $\boldsymbol{p}_i\,(\boldsymbol{p}_f)$ and $\varepsilon_i\,(\varepsilon_f)$ are, respectively, the initial (final) momentum and energy and U is the imperfection-perturbation. We assume a constant absolute squared matrix-elements $\mathcal{M}^2$. The current density $j_c^{(i)}$ along the c-axis due to a group of particles i having charge $q^{(i)}$ and momentum-energy $(\boldsymbol{p}, \varepsilon)$ is calculated from

$$j_c^{(i)} = j_{c,H}^{(i)} - j_{c,L}^{(i)} = q^{(i)} a_0 w n^{(i)} \left(v_H^{(i)} - v_L^{(i)} \right), \tag{34}$$

where $n^{(i)}$ is the 2D number density, a_0 the interlayer distance, and $j_{c,H}^{(i)}\left(j_{c,L}^{(i)}\right)$ represents the current density from the high (low)-temperature end. Pairons move with the same speed $c = (2/\pi)v_F$, but the velocity component v_x is

$$v_x = \frac{\partial \varepsilon}{\partial p_x} = \frac{c p_x}{p} = \frac{c^2}{\varepsilon} p_x. \tag{35}$$

Lower-energy (smaller p) pairons are more likely to get trapped by the imperfection and going into tunneling. We represent this tendency by $K = B/\varepsilon$, where B is a constant having the dimension of energy/length. Since the thermal average of the v is different, a steady current is generated. The temperature difference $\Delta T\,(= T_{\mathrm{H}} - T_{\mathrm{L}})$ causes a change in the B-E distribution F:

$$F(\varepsilon) \equiv \left[e^{(\varepsilon-\mu)\beta} + 1\right]^{-1}, \quad \beta \equiv (k_{\mathrm{B}}T)^{-1}, \tag{36}$$

where μ is the chemical potential. We compute the current density j_{c} from

$$j_{\mathrm{c}} = 2e\frac{\mathcal{M}^2 B}{\hbar^3 c^2}\frac{a_0 \Delta T}{k_{\mathrm{B}}T^2}\int_0^{cp_0} \mathrm{d}\varepsilon\, \frac{\mathrm{d}F(\varepsilon)}{\mathrm{d}\beta}, \tag{37}$$

assuming a small ΔT. Not all pairons reaching an imperfection are triggered into tunneling. The factor B contains this correction.

At the BEC temperature (T_{c}), the chemical potential μ vanishes:

$$\mu(T_{\mathrm{c}}) = 0, \tag{38}$$

and

$$\beta\mu \equiv \mu/k_{\mathrm{B}}T \tag{39}$$

is negative and small in magnitude for $T > T_{\mathrm{c}}$. For high temperature and low density, the B-E distribution function F can be approximated by the Boltzmann distribution function:

$$F(\varepsilon) \approx f_0(\varepsilon) = \exp(\mu - \varepsilon)\beta, \tag{40}$$

which is normalized such that

$$\frac{1}{(2\pi\hbar)^2}\int \mathrm{d}^2 p f_0(\varepsilon) = n_0 \ \left(\text{pairon density}\right). \tag{41}$$

All integrals in (37) and (41) can be evaluated simply by using $\int_0^\infty \mathrm{d}x e^{-x}x^n = n!$. Hence we obtain

$$\int \mathrm{d}^2 p f_0(\varepsilon) = 2\pi m \int_0^\infty \mathrm{d}\varepsilon e^{\beta\mu} e^{-\beta\varepsilon} = 2\pi m e^{\mu\beta}\beta^{-1}. \tag{42}$$

The integral in (37) is then calculated as

$$\int_0^{cp_0} \mathrm{d}\varepsilon\, \frac{\mathrm{d}F(\varepsilon)}{\mathrm{d}\beta} \approx \int_0^{cp_0} \mathrm{d}\varepsilon\, \frac{\mathrm{d}}{\mathrm{d}\beta} f_0(\varepsilon) = e^{\mu\beta}\int_0^\infty \mathrm{d}\varepsilon\, \varepsilon e^{-\beta\varepsilon} = e^{\beta\mu}\beta^{-2}. \tag{43}$$

From Eqs. (11) and (37) along with Eq. (43), we obtain

$$A_{\mathrm{c}} \sim 2e\mathcal{M}^2 B k_{\mathrm{B}} a_0 \left(\hbar^3 c^2\right)^{-1}, \tag{44}$$

which is T-independent.

Experiments [5] indicate that the first term $C_1\rho_{\mathrm{ab}}$ in (31) is dominant for $\mathrm{x} > 6.8$:

$$\rho_{\mathrm{c}} \sim C_1\rho_{\mathrm{ab}} \propto T. \tag{45}$$

Hence at x = 7, we have an expression for the out-of-plane Seebeck coefficient S_c above the critical temperature:

$$S_c \equiv \frac{A_c}{\sigma_c} = A_c C_1 \rho_{ab} \propto T > 0. \ (\rho_{ab} \propto T). \tag{46}$$

The lower the temperature of the initial state, the tunneling occurs more frequently. The particle current runs from the low- to the high-temperature end, the opposite direction to that of the conduction in the ab-plane. Hence $S_c > 0$, which is in accord with experiments (see **Figure 1**).

6. Resistivity above the critical temperature

We use simple kinetic theory to describe the transport properties [22]. Kinetic theory was originally developed for a dilute gas. Since a conductor is far from being the gas, we shall discuss the applicability of kinetic theory. The Bloch wave packet in a crystal lattice extends over one unit cell, and the lattice-ion force averaged over a unit cell vanishes. Hence the conduction electron ("electron," "hole") runs straight and changes direction if it hits an impurity or phonon (wave packet). The electron–electron collision conserves the net momentum, and hence, its contribution to the conductivity is zero. Upon the application of a magnetic field, the system develops a Hall electric field so as to balance out the Lorentz magnetic force on the average. Thus, the electron still move straight and is scattered by impurities and phonons, which makes the kinetic theory applicable.

YBCO is a "hole"-type HTSC in which "holes" are the majority carriers above T_c, while $Nd_{1.84}Ce_{0.16}$ CuO_4 is an "electron"-type HTSC.

6.1 In-plane resistivity

Consider a system of "holes," each having effective mass m_2^* and charge $+e$, scattered by phonons. Assume a weak electric field $\boldsymbol{E}$ applied along the x-axis. Newton's equation of motion for the "hole" with the neglect of the scattering is

$$m_2^* \frac{\mathrm{m}dv_x}{\mathrm{d}t} = eE. \tag{47}$$

Solving it for v_x and assuming that the acceleration persists in the mean-free time τ_2, we obtain

$$v_d = \frac{eE}{m_2^*} \tau_2 \tag{48}$$

for the drift velocity v_d. The current density (x-component) j is given by

$$j = en_2 v_d = n_2 \frac{e^2 \tau_2}{m_2^*} E, \tag{49}$$

where n_2 is the "hole" density. Assuming Ohm's law

$$j = \sigma E, \tag{50}$$

we obtain an expression for the electrical conductivity:

$$\sigma_2 = \frac{n_2 e^2}{m_2^*} \frac{1}{\Gamma_2}, \tag{51}$$

where $\Gamma_2 \equiv \tau_2^{-1}$ is the scattering rate. The phonon scattering rate can be computed, using

$$\Gamma_2 = n_{\text{ph}} v_{\text{F}} A_2, \tag{52}$$

where A_2 is the scattering diameter. If acoustic phonons having average energies

$$\langle \hbar\omega_q \rangle \equiv \alpha_0 \hbar\omega_{\text{D}} \ll k_{\text{B}} T, \quad \alpha_0 \sim 0.20 \tag{53}$$

are assumed, then the phonon number density n_{ph} is given by [23].

$$n_{\text{ph}} = n_{\text{a}} [\exp(\alpha_0 \hbar\omega_{\text{D}} / k_{\text{B}} T) - 1]^{-1} \simeq n_{\text{a}} \frac{k_{\text{B}} T}{\alpha_0 \hbar\omega_{\text{D}}}, \tag{54}$$

where

$$n_{\text{a}} \equiv (2\pi)^{-2} \int \text{d}^2 k \tag{55}$$

is the small $\boldsymbol{k}$-space area where the acoustic phonons are located.
Using Eqs. (51), (52), and (54), we obtain

$$\sigma_2 = \frac{C_2 n_2 e^2}{T}, \quad C_2 \equiv \frac{\alpha_0 \hbar\omega_{\text{D}}}{n_{\text{a}} m_2^* k_{\text{B}} v_{\text{F}} A_2}. \tag{56}$$

Similar calculations apply to "electrons." We obtain

$$\sigma_1 = \frac{C_1 n_1 e^2}{T}, \quad C_1 \equiv \frac{\alpha_0 \hbar\omega_{\text{D}}}{n_{\text{a}} m_1^* k_{\text{B}} v_{\text{F}} A_2}. \tag{57}$$

The resistivity ρ is the inverse of the conductivity σ. Hence the resistivity for YBCO is proportional to the temperature T:

$$\rho \equiv \frac{1}{\sigma} \propto T. \tag{58}$$

Let us now consider a system of + pairons, each having charge $+2e$ and moving with the linear dispersion relation:

$$\varepsilon = cp. \tag{59}$$

Since

$$v_x = (\text{d}\varepsilon/\text{d}p)(\partial p/\partial p_x) = c\,(p_x/p), \tag{60}$$

Newton's equation of motion is

$$\frac{p}{c} \frac{\text{d}v_x}{\text{d}t} = \frac{\varepsilon}{c^2} \frac{\text{d}v_x}{\text{d}t} = 2eE, \tag{61}$$

yielding $v_x = 2e(c^2/\varepsilon)Et +$initial velocity. After averaging over the angles, we obtain

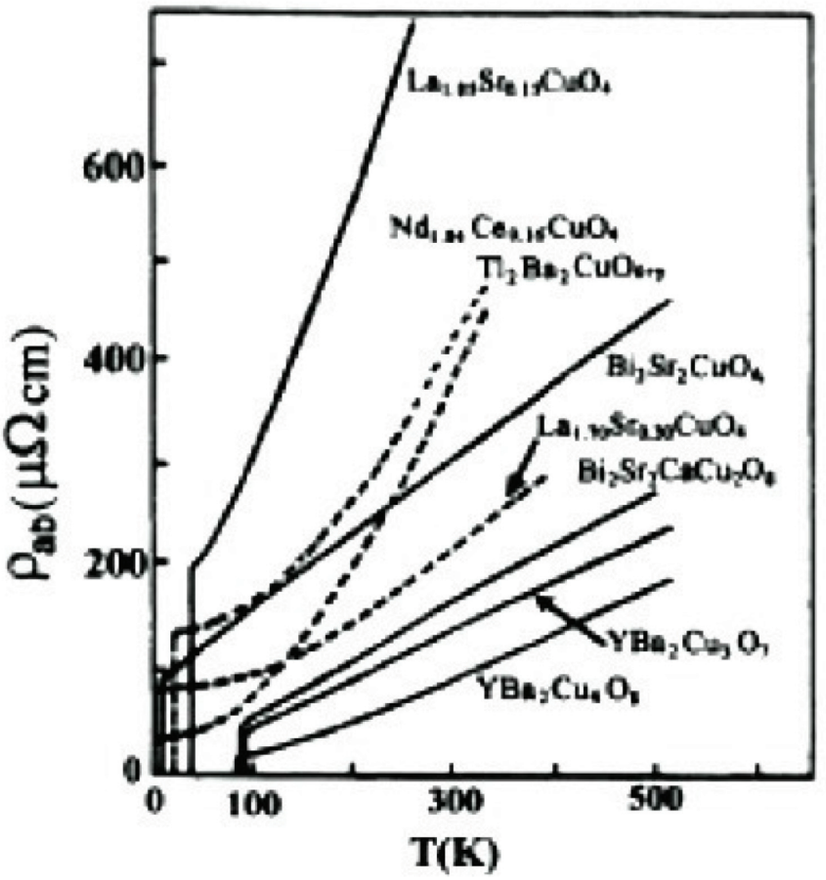

Figure 8.
Resistivity in the ab plane, ρ_{ab} vs. temperature T. Solid lines represent data for HTSC at optimum doping and dashed lines data for highly overdosed samples, after Iye [24].

$$v_d^{(3)} = 2ec^2\tau_3 E\langle\varepsilon^{-1}\rangle, \tag{62}$$

where τ_3 is the pairon mean free time and the angular brackets denote a thermal average. Using this and Ohm's law, we obtain

$$\sigma_3 = (2e)^2 c\langle\varepsilon^{-1}\rangle n_3\Gamma_3^{-1}, \quad \Gamma_3 \equiv \tau_3^{-1}, \tag{63}$$

where n_3 is the pairon density and Γ_3 is the pairon scattering rate. If we assume a Boltzmann distribution for bosonic pairons above T_c, then we obtain

$$\begin{aligned}\langle\varepsilon^{-1}\rangle &\equiv \left(\frac{2\pi}{(2\pi\hbar)^2}\int_0^\infty dpp\,\frac{1}{\varepsilon}e^{\beta cp}\right)\left(\frac{2\pi}{(2\pi\hbar)^2}\int_0^\infty dpp\,e^{\beta cp}\right)^{-1} \\ &= (k_B T)^{-1} \quad \text{for} \quad T > T_c.\end{aligned} \tag{64}$$

The rate Γ_3 is calculated with the assumption of a phonon scattering. We then obtain

$$\sigma_3 = \frac{4n_3e^2c^2}{k_B T\Gamma_3} = \frac{2n_2e^2C_3}{T^2}, \qquad C_3 \equiv \frac{8}{\pi^2}\frac{\alpha_0\hbar\omega_D v_F}{n_a k_B^2 A_3}. \tag{65}$$

The total conductivity σ for YBCO is $\sigma_2 + \sigma_3$. Thus taking the inverse of σ, we obtain, by using the results (56) and (65):

$$\rho_{ab} \equiv \frac{1}{\sigma} = \left(\frac{C_2 n_2 e^2}{T} + \frac{C_3 n_3 2e^2}{T^2}\right)^{-1} = \frac{T^2}{n_2 e^2 (C_2 T + 2C_3)} \tag{66}$$

while the conductivity for $Nd_{1.84}Ce_{0.16}CuO_4$ is given by $\sigma_1 + \sigma_3$, and hence the resistivity is similarly given by

$$\rho_{ab} = \frac{T^2}{n_1 e^2 (C_1 T + 2C_3)}. \tag{67}$$

In $Nd_{1.84}Ce_{0.16}$ while in $YCuO_4$ system, "electrons" and − pairons play an essential role for the conduction. In $YBa_2Cu_3O_{7-\delta}$ the "holes" and + pairons are the major carriers in the in-plane resistivity. The resistivity in the plane (ρ_{ab}) vs. temperature (T) in various samples at optimum doping after Iye [24] is shown in **Figure 8**. The overall data are consistent with our formula.

At higher temperature (>160 K), the resistivity ρ_{ab} is linear (see formula (58)):

$$\rho_{ab} \propto T, \quad T > 160 \text{ K}, \tag{68}$$

in agreement with experiments (**Figure 8**). This part arises mainly from the conduction electrons scattered by phonon. At the low temperatures close to the critical temperature T_c, the in-plane resistivity ρ_{ab} shows a T-quadratic behavior [see formula (66)]:

$$\rho_{ab} \propto T^2 \quad (\text{near and above } T_c). \tag{69}$$

This behavior arises mainly from the pairons scattered by phonons. The agreement with the data represents one of the most important experimental supports for the BEC picture of superconductivity.

Author details

Shigeji Fujita[1] and Akira Suzuki[2*]

1 Department of Physics, University at Buffalo, SUNY, Buffalo, NY, USA

2 Department of Physics, Tokyo University of Science, Tokyo, Japan

*Address all correspondence to: asuzuki@rs.kagu.tus.ac.jp

References

[1] Bednorz JG, Müller KA. Zeitschrift für Physik B Condensed Matter. 1986; **64**:189

[2] Halley JW, editor. Theory of High Temperature Superconductivity. Redwood City, CA: Addison-Wesley; 1988

[3] Lundquist S, editor. Towards the Theoretical Understanding of High-T Superconductivity. Singapore: World Scientific; 1988

[4] Wu MK, Ashburn JR, Torng CJ, Hor PH, Meng RL, Gao L, et al. Physical Review Letters. 1987;**58**:908

[5] Terasaki I, Saito Y, Tajima S, Miyamoto S, Tanaka S. Physica C. 1994; **235-240**:1413

[6] Terasaki I, Sato Y, Tajima S, Miyamoto S, Tanaka S. Physical Review B. 1995;**52**:16246

[7] Farrell DE, Beck RG, Booth MF, Allen CJ, Bukowski ED, Ginsberg DM. Physical Review B. 1990;**42**:6758

[8] Godoy S, Fujita S. Journal of Engineering Science. 1991;**29**:1201

[9] Kitazawa K, Ishiguro T, editors. Advances in Superconductivity. Tokyo: Springer; 1989

[10] Yukawa H. Proceedings of the Physico-Mathematical Society of Japan. 1935;**17**:48

[11] Bardeen J, Cooper LN, Schrieffer JR. Physics Review. 1957;**108**:1175

[12] Cooper LN. Physics Review. 1956; **104**:1189

[13] Fujita S, Ito K, Godoy S. Quantum Theory of Conducting Matter, Superconductivity. New York: Springer; 2009

[14] Lanzara A, Bogdanov PV, Zhou XJ, Kellar SA, Feng DL, Lu ED, et al. Nature. 2001;**412**:510

[15] Loram JW, Mirza KA, Cooper JR, Liang WY. Journal of Superconductivity. 1994;**7**:347

[16] Fujita S, Godoy S, Nguyen D. Foundations of Physics. 1995;**25**:1209

[17] Terasaki I, Sato Y, Terajima S. Physical Review B. 1997;**55**:15300

[18] Terasak I, Sato Y, Tajima S. Journal of the Korean Physical Society. 1994; **31**:23

[19] Takenaka K, Mizuhashi K, Takagi H, Uchida S. Physical Review B. 1994;**50**: 6534

[20] Fujita S, Tamura Y, Suzuki A. Modern Physics Letters B. 2000;**14**:30

[21] Fujita S, Godoy S. Theory of High Temperature Superconductivity. The Netherlands: Kluwer Academic; 2001. pp. 65-69, p. 108

[22] Fujita S, Kim SY-G, Okamura Y. Modern Physics Letters B. 2000;**14**:495

[23] Chien TR, Wang ZZ, Ong NP. Physical Review Letters. 1991;**67**:2088

[24] Iye Y. In: Ginzberg DM, editor. Physical Properties of High Temperature Superconductors III. Singapore: World Scientific; 1989